

Comparative Analysis of SMC-LMI and LQR Controllers for Double Inverted Pendulum

Ma-Sieu Phan¹, Thanh-Cong Do¹, Van-Quy Truong¹ and Thi-Van-Anh Nguyen^{1,*}

¹Hanoi University of Science and Technology, Hanoi, Vietnam

*Corresponding author E-mail: anh.nguyenthivan1@hust.edu.vn

Abstract

This paper introduces an innovative method for achieving stability of the highly nonlinear and unstable double inverted pendulum using a combination of linear matrix inequality (LMI) techniques and sliding mode control (SMC). Sliding mode control is a widely used technique for stabilizing the highly unstable and nonlinear double inverted pendulum system. The LMI-based approach is well-suited for handling system uncertainties and constraints, making it a potent tool for robust control design. Compared to other nonlinear control methods, the LMI approach is more computationally efficient and simpler to implement. The controller proposed in this study is evaluated alongside the Linear Quadratic Regulator (LQR) controller to demonstrate its superior performance. The simulation results obtained through the proposed controller demonstrate its effectiveness in stabilizing the double inverted pendulum.

Keywords: Linear matrix inequality, Sliding mode control, LQR control, stabilization control, Double inverted pendulum.

Abbreviations

SMC	Sliding Mode Control
LMI	Linear Matrix Inequality
LQR	Linear Quadratic Regulator

1. Introduction

The double inverted pendulum is a highly unstable and nonlinear system that is widely used in research to study the dynamics and control of complex systems [1], [2], [3]. Comprising two pendulums connected by a hinge, the motion of the first pendulum influences the motion of the second pendulum. Due to its highly sensitive nature, the double inverted pendulum is a challenging system to control using conventional linear control methods. Nevertheless, it presents an ideal tested for developing and evaluating advanced control algorithms. The double inverted pendulum has numerous applications in various fields, such as aerospace, robotics, and industrial automation. It is used in aerospace to analyze the dynamics of flight control systems, while in robotics, it is used to develop sophisticated control algorithms for multi-jointed robotic arms and legs. The double inverted pendulum is also utilized in industrial automation to evaluate and create control algorithms for complex manufacturing processes. It is a significant and versatile system that has extensive applications in both research and industry. Controlling a double inverted pendulum is a complex task, given its nonlinear and unstable nature. To stabilize this system, researchers have explored various control methods. One of the

widely-used control techniques for double inverted pendulum stabilization is sliding mode control (SMC) [4], [5], [6]. This method involves designing a sliding surface that guides the system to a desired state. The control signal is then formulated to ensure the system stays on the sliding surface, ensuring robustness against external disturbances and modeling errors. Another popular method is the Linear Quadratic Regulator (LQR) control algorithm, which is a classical linear control method based on a quadratic cost function [7], [8], [9]. This technique determines the optimal control action by minimizing the cost function, which is a weighted sum of the system state error and the control input. While LQR control is limited to linear systems, it provides a straightforward means of designing a feedback control system that stabilizes the double inverted pendulum. Recently, researchers have combined SMC with linear matrix inequality (LMI) control methods for controlling a nonlinear system [10] or wind-energy conversion system [11]. Recognizing the merits and feasibility of applying the combined approach of sliding mode control and linear matrix inequality to systems characterized by high nonlinearity, we have implemented this methodology for stable control of the double inverted pendulum.

This paper focuses on the effectiveness of a combined sliding controller and linear matrix inequality (LMI) approach for stabilizing the double inverted pendulum. LMI is a valuable technique for designing controllers in nonlinear systems like the inverted pendulum, as it enables the formulation of control design problems as convex optimization problems. The LMI-based approach is well-suited to handle system uncertainties

and constraints commonly encountered in practical systems, providing robust stability and performance guarantees even in the presence of model uncertainties and disturbances. Moreover, the LMI approach allows for the design of controllers with specific performance criteria, such as minimizing control effort or settling time. In comparison to alternative nonlinear control methods like adaptive control or fuzzy logic control [12],[13], the LMI approach is computationally efficient and relatively simple to implement. This advantage stems from solving a set of linear matrix inequalities, which can be efficiently addressed using existing numerical optimization tools. The LMI approach offers computational efficiency by consolidating multiple conditions into a single linear matrix inequality, reducing computational complexity. This simplification enables efficient representation and manipulation of the control design problem. Additionally, the LMI approach leverages existing tools like MATLAB or the Yalmip toolbox, which provide dedicated functionalities for converting mechanical conditions into linear matrix inequalities. The paper aims to demonstrate the superior performance of the proposed controller for stabilizing the double inverted pendulum by conducting a thorough analysis and comparing the results with those obtained using the LQR controller.

The upcoming sections of the paper will cover various aspects of the proposed control strategy for the inverted pendulum. The second part will introduce the model of the double inverted pendulum, while the third section will discuss the LQR controller. The fourth section will elaborate on the proposed sliding mode controller combined with linear matrix inequality theory. The fifth section will present the simulation results obtained through the proposed controller. Lastly, the conclusion will summarize the findings and contributions of the paper.

2. Double inverted pendulum Modeling

The double inverted pendulum is a mechanical system consisting of two pendulums connected in series, where each pendulum is free to rotate about its pivot point, see Figure 1. In this system, θ_1 and θ_2 represent the deflections of the first and second pendulums from the vertical, respectively. Meanwhile, y represents the displacement of the cart. The parameters of the double inverted pendulum include the lengths of the pendulums, denoted as L_1 and L_2 , which determine the distance from the pivot points to the respective masses. The masses of the pendulums, represented as m_1 and m_2 , signify the amount of mass concentrated at each pendulum's center of mass. The moment of inertia of each pendulum, denoted as J_1 and J_2 , characterizes the distribution of mass and shape of the pendulum. In the double inverted pendulum on a cart model, the calculation of energy involves considering the kinetic energy of the cart and two pendulums, as well as the potential energy due to the height of the pendulums. The system modeling process has also been detailed in [14].

The kinetic energy of the cart is expressed as follows:

$$T_0 = \frac{1}{2} m_0 \dot{y}^2. \quad (1)$$

The kinetic energy of the first pendulum:

$$T_1 = \frac{1}{2} m_1 [\dot{y} + \dot{\theta}_1 l_1 \cos(\theta_1)]^2 + \frac{1}{2} m_1 \dot{\theta}_1^2 l_1^2 \sin^2 \theta_1 + \frac{1}{2} J_1 \dot{\theta}_1^2. \quad (2)$$

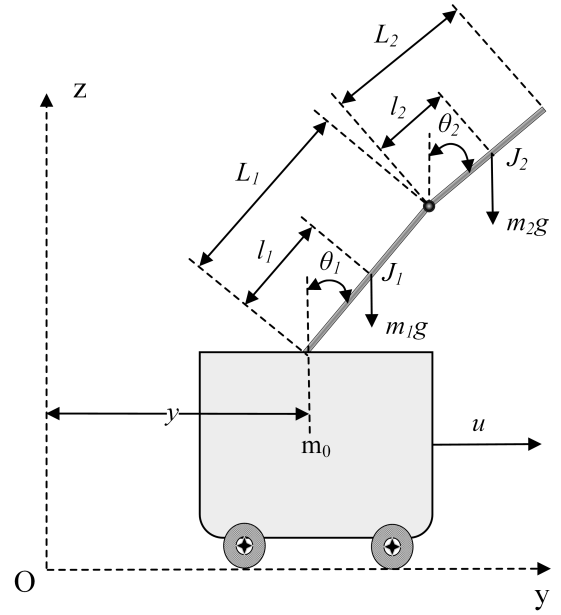


Figure 1. Double inverted pendulum.

The kinetic energy of the second pendulum:

$$T_2 = \frac{1}{2} m_2 [\dot{y} + \dot{\theta}_1 l_1 \cos \theta_1 + \dot{\theta}_2 l_2 \cos \theta_2]^2 + \frac{1}{2} m_2 [\dot{\theta}_1 L_1 \sin \theta_1 + \dot{\theta}_2 L_2 \sin \theta_2]^2 + \frac{1}{2} J_2 \dot{\theta}_2^2. \quad (3)$$

The expression for the total kinetic energy is as follows:

$$T = T_0 + T_1 + T_2,$$

$$T = \frac{1}{2} (m_0 + m_1 + m_2) \dot{y}^2 + \frac{1}{2} (m_1 l_1^2 + m_2 L_1^2 + J_1) \dot{\theta}_1^2 + \frac{1}{2} (m_2 l_2^2 + J_2) \dot{\theta}_2^2 + (m_1 l_1 + m_2 L_1) \dot{y} \dot{\theta}_1 \cos \theta_1 + m_2 l_2 \dot{y} \dot{\theta}_2 \cos \theta_2 + m_2 L_1 l_2 \cos(\theta_1 - \theta_2) \dot{\theta}_1 \dot{\theta}_2. \quad (4)$$

The potential energy of the cart:

$$V_0 = 0 \quad (5)$$

The potential energy of the first pendulum:

$$V_1 = m_1 g l_1 \cos \theta_1 \quad (6)$$

The potential energy of the second pendulum:

$$V_2 = m_2 g (L_1 \cos \theta_1 + l_2 \cos \theta_2) \quad (7)$$

The total potential energy is calculated as follows:

$$V = (m_1 l_1 + m_2 L_1) g \cos \theta_1 + m_2 l_2 g \cos \theta_2 \quad (8)$$

The expression for the Lagrange function is given as follows:

$$L = \frac{1}{2} (m_0 + m_1 + m_2) \dot{y}^2 + \frac{1}{2} (m_1 l_1^2 + m_2 L_1^2 + J_1) \dot{\theta}_1^2 + \frac{1}{2} (m_2 l_2^2 + J_2) \dot{\theta}_2^2 + (m_1 l_1 + m_2 L_1) \dot{y} \dot{\theta}_1 \cos \theta_1 + m_2 l_2 \dot{y} \dot{\theta}_2 \cos \theta_2 + m_2 L_1 l_2 \cos(\theta_1 - \theta_2) \dot{\theta}_1 \dot{\theta}_2 - (m_1 l_1 + m_2 L_1) g \cos \theta_1 - m_2 l_2 g \cos \theta_2 \quad (9)$$

By taking the derivative of the Lagrange function, we obtain the dynamic equations:

$$u = (m_0 + m_1 + m_2)\ddot{y} + (m_1l_1 + m_2L_1)\ddot{\theta}_1\cos\theta_1 + m_2l_2\ddot{\theta}_2\cos\theta_2 - (m_1l_1 + m_2L_1)\dot{\theta}_1^2\sin\theta_1 - m_2l_2\dot{\theta}_2^2\sin\theta_2 \quad (10)$$

$$0 = (m_1l_1^2 + m_2L_1^2 + J_1)\ddot{\theta}_1 + (m_1l_1 + m_2L_1)\ddot{y}\cos\theta_1 + m_2L_1l_2\cos(\theta_1 - \theta_2)\ddot{\theta}_2 + m_2L_1l_2\sin(\theta_1 - \theta_2)\dot{\theta}_2^2 - (m_1l_1 + m_2L_1)g\sin\theta_1 \quad (11)$$

$$0 = (m_2l_2^2 + J_2)\ddot{\theta}_2 + m_2l_2\ddot{y}\cos\theta_2 + m_2L_1l_2\cos(\theta_1 - \theta_2)\ddot{\theta}_1 - m_2L_1l_2\sin(\theta_1 - \theta_2)\dot{\theta}_1^2 - m_2l_2g\sin\theta_2 \quad (12)$$

Note that:

$$a_0 = m_0 + m_1 + m_2$$

$$a_1 = m_1l_1 + m_2L_1$$

$$a_2 = m_1l_1^2 + m_2L_1^2 + J_1$$

$$a_3 = m_2l_2$$

$$a_4 = m_2L_1l_2$$

$$a_5 = m_2l_2^2 + J_2$$

The dynamic equation can be rewritten as follows:

$$u = a_0\ddot{y} + a_1\ddot{\theta}_1\cos\theta_1 + a_3\ddot{\theta}_2\cos\theta_2 - a_1\dot{\theta}_1^2\sin\theta_1 - a_3\dot{\theta}_2^2\sin\theta_2 \quad (13)$$

$$0 = a_1\ddot{y}\cos\theta_1 + a_2\ddot{\theta}_1 + a_4\ddot{\theta}_2\cos(\theta_1 - \theta_2) + a_4\dot{\theta}_2^2\sin(\theta_1 - \theta_2) - a_1g\sin\theta_1 \quad (14)$$

$$0 = a_3\ddot{y}\cos\theta_2 + a_4\ddot{\theta}_1\cos(\theta_1 - \theta_2) + a_5\ddot{\theta}_2 - a_4\sin(\theta_1 - \theta_2)\dot{\theta}_1^2 - a_3g\sin\theta_2 \quad (15)$$

3. LQR Control

This section focuses on the application of LQR control technique for stabilizing the double inverted pendulum system. LQR control is a widely used optimal control strategy that aims to minimize a quadratic cost function while ensuring system stability. We set the variables as follows: $x_1 = y, x_2 = \dot{y}, x_3 = \theta_1, x_4 = \dot{\theta}_1, x_5 = \theta_2, x_6 = \dot{\theta}_2$. The system is linearized around the operating point $x = 0$ to obtain a linearized equation.

$$\dot{x} = Ax + Bu \quad (16)$$

with $x = (x_1, x_2, x_3, x_4, x_5, x_6)^T$.

$$A = \begin{pmatrix} 0 & 1 & 0 & 0 & 0 & 0 \\ \frac{\partial f(\dot{y})}{\partial x_1} & \frac{\partial f(\dot{y})}{\partial x_2} & \frac{\partial f(\dot{y})}{\partial x_3} & \frac{\partial f(\dot{y})}{\partial x_4} & \frac{\partial f(\dot{y})}{\partial x_5} & \frac{\partial f(\dot{y})}{\partial x_6} \\ 0 & 0 & 0 & 1 & 0 & 0 \\ \frac{\partial f(\dot{\theta}_1)}{\partial x_1} & \frac{\partial f(\dot{\theta}_1)}{\partial x_2} & \frac{\partial f(\dot{\theta}_1)}{\partial x_3} & \frac{\partial f(\dot{\theta}_1)}{\partial x_4} & \frac{\partial f(\dot{\theta}_1)}{\partial x_5} & \frac{\partial f(\dot{\theta}_1)}{\partial x_6} \\ 0 & 0 & 0 & 0 & 0 & 1 \\ \frac{\partial f(\dot{\theta}_2)}{\partial x_1} & \frac{\partial f(\dot{\theta}_2)}{\partial x_2} & \frac{\partial f(\dot{\theta}_2)}{\partial x_3} & \frac{\partial f(\dot{\theta}_2)}{\partial x_4} & \frac{\partial f(\dot{\theta}_2)}{\partial x_5} & \frac{\partial f(\dot{\theta}_2)}{\partial x_6} \end{pmatrix}$$

$$B = \begin{pmatrix} 0 \\ \frac{\partial f(\dot{y})}{\partial u} \\ 0 \\ \frac{\partial f(\dot{\theta}_1)}{\partial u} \\ 0 \\ \frac{\partial f(\dot{\theta}_2)}{\partial u} \end{pmatrix}$$

By substituting the operating point $x = 0$, we obtain the following matrix:

$$A = \begin{pmatrix} 0 & 1 & 0 & 0 & 0 & 0 \\ 0 & 0 & -6.3 & 0 & 0 & 0 \\ 0 & 0 & 0 & 1 & 0 & 0 \\ 0 & 0 & 70 & 0 & -8.9091 & 0 \\ 0 & 0 & 0 & 0 & 0 & 1 \\ 0 & 0 & -49 & 0 & 41.0808 & 0 \end{pmatrix}; B = \begin{pmatrix} 0 \\ 1.073 \\ 0 \\ -3.896 \\ 0 \\ 0.5051 \end{pmatrix}$$

The control equation is expressed as follows:

$$u^* = -Kx \quad (17)$$

We have:

$$J = \int_0^\infty (x^T Qx + u^T Ru) dt \quad (18)$$

with $Q = Q^T \geq 0, R = R^T > 0$.

The objective is to identify the matrix K that minimizes the loss function J . The optimal matrix K , obtained from the Riccati equation, takes the following form:

$$K = R^{-1}B^T P \quad (19)$$

Consequently, the control signal u will be of the form:

$$u = -Kx = -R^{-1}B^T Px, \quad (20)$$

where $K = lqr(A, B, Q, R)$. The matrix P is the solution to the Riccati algebraic equation.

$$PA + A^T P + Q - PBR^{-1}B^T P = 0. \quad (21)$$

4. Sliding mode control based LMI

In this section, we explore the application of sliding mode control and linear inequality matrix techniques for controlling the double inverted pendulum system. Sliding mode control is a robust control approach known for its ability to handle uncertainties and disturbances in dynamic systems. Additionally, we incorporate a linear inequality matrix to impose constraints which can stay within predefined bounds. The combined use of sliding mode control and linear inequality matrix provides a promising approach for addressing the control challenges associated with the double inverted pendulum system, and we investigate its effectiveness and performance in this section. The equation (16) is rewritten in the presence of disturbance:

$$\dot{x}(t) = Ax(t) + B(u + f(t)) \quad (22)$$

with $|f(t)| \leq \delta_f$, and δ_f is a positive constant. The choice of the sliding variable s is determined by the following equation:

$$s = B^T Px, \quad (23)$$

where P is positive definite matrix with dimensions 6×6 . The control signal is expressed in the following form:

$$u(t) = u_{eq} + u_n, \quad (24)$$

where $u_{eq} = -(B^T PB)^{-1} B^T PAx(t)$,
 $u_n = -(B^T PB)^{-1} (|B^T PB| \delta_f + \varepsilon_0) sgn(s)$ and $\varepsilon_0 > 0$.
 The Lyapunov function is selected in the following manner:

$$V = \frac{1}{2} s^2. \quad (25)$$

$$\begin{aligned} \dot{s} &= B^T P \dot{x}(t) = B^T P (Ax(t) + B(u + f(t))) \\ &= B^T PAx(t) + B^T PBu + B^T PBf(t) \\ &= B^T PAx(t) + B^T PB(- (B^T PB)^{-1} B^T PAx(t) \\ &\quad - (B^T PB)^{-1} (|B^T PB| \delta_f + \varepsilon_0) sgn(s)) + B^T PBf(t) \\ &= -(|B^T PB| \delta_f + \varepsilon_0) sgn(s) + B^T PBf(t). \end{aligned}$$

Then:

$\dot{V} = s \dot{s} = -(|B^T PB| \delta_f + \varepsilon_0) |s| + B^T PBf(t) \leq -\varepsilon_0 |s|$. The controller is designed as follows to determine the symmetric matrix P :

$$u(t) = -Kx + v(t), \quad (26)$$

with $v(t) = Kx + u_{eq} + u_n$.

There exists a matrix K such that $\bar{A} = A - BK$ is stable, leading to the following expression:

$$\dot{x}(t) = \bar{A}x(t) + B(v + f(t)), \quad (27)$$

where K represents a 1×6 vector.

The selection of the Lyapunov function is as follows:

$$V = x^T Px, \quad (28)$$

Then:

$$\dot{V} = 2x^T P \dot{x} = 2x^T P (\bar{A}x(t) + B(v + f(t))) = 2x^T P \bar{A}x(t) + 2x^T PB(v + f(t)).$$

When $t \geq t_0$, it exists $s = B^T Px(t) = 0$, or $s^T = x^T PB = 0$, we obtain:

$$\dot{V} = 2x^T P \bar{A}x = x^T (P \bar{A} + \bar{A}^T P)x = 2x^T Mx.$$

For $\dot{V} < 0, M < 0$, we have: $P \bar{A} + \bar{A}^T P < 0$

As the matrix \bar{A} is Hurwitz, it is feasible to fulfill the condition $P \bar{A} + \bar{A}^T P < 0$. By multiplying the aforementioned inequality by P^{-1} , we obtain:

$$\bar{A}P^{-1} + P^{-1}\bar{A}^T < 0$$

We denote $X = P^{-1}$:

$$\bar{A}X + X\bar{A}^T < 0$$

$$(A - BK)X + X(A - BK)^T < 0$$

Note that $L = KX$, we have:

$$AX - BL + XA^T - L^T B^T < 0 \quad (29)$$

To ensure that P is a symmetric matrix in the Linear Matrix Inequality (LMI), we design:

$$P = P^T \text{ or } X = X^T \quad (30)$$

Table 1. Parameter table of the double inverted pendulum system.

Symbol	Notation	Value	Unit
m_0	Mass of the cart	0.8	kg
m_1	Mass of the first pendulum	0.5	kg
m_2	Mass of the second pendulum	0.3	kg
L_1	Length of the first pendulum	0.3	m
L_2	Length of the second pendulum	0.2	m
l_1	Distance to center of gravity of first pendulum	0.15	m
l_2	Distance to center of gravity of second pendulum	0.1	m
J_1	The moment of inertia of the first pendulum	0.006	kgm ²
J_2	The moment of inertia of the second pendulum	0.006	kgm ²
g	Gravity acceleration	9.8	m/s ²

5. Simulation results

In this section, we present the simulation results obtained from applying sliding mode control based on LMI and LQR control techniques to the control of the double inverted pendulum system. The performance of both control strategies is evaluated and compared in terms of stability for showing the effectiveness of the proposed control approaches. Initial conditions for the state variables are chosen as $y = 0.1(m)$, $\theta_1 = \theta_2 = \frac{\pi}{12}$ and $\dot{y} = \dot{\theta}_1 = \dot{\theta}_2 = 0$. The presented below is a table containing the parameter values of the double inverted pendulum model, see Table 1 [14]. The matrix Q and R are selected as follows:

$$Q = \text{diag}(1 \ 1 \ 10 \ 100 \ 10 \ 100), R = 1.$$

The utilization of LMI aims to obtain a positive definite matrix. Unlike the conventional sliding controller that requires adjusting sliding surface parameters accordingly, the use of LMI enables a more straightforward and convenient approach by directly specifying the matrix. This methodology streamlines the process of determining the sliding surface, making it easier to implement and allowing for greater convenience in control design. We obtain:

$$K = [\ 1 \ 3.0595 \ -188.6554 \ -9.2430 \ 213.9421 \ 35.1107 \]$$

and

$$P =$$

$$\begin{bmatrix} 0.0336 & 0.0310 & -0.1406 & 0.0078 & 0.3251 & 0.0673 \\ 0.0310 & 0.0885 & -0.3796 & 0.0225 & 0.7425 & 0.1724 \\ -0.1406 & -0.3796 & 6.2744 & 0.0351 & -8.7704 & -1.2776 \\ 0.0078 & 0.0225 & 0.0351 & 0.0224 & 0.0347 & 0.0183 \\ 0.3251 & 0.7425 & -8.7704 & 0.0347 & 13.7654 & 2.2191 \\ 0.0673 & 0.1724 & -1.2776 & 0.0183 & 2.2191 & 0.5075 \end{bmatrix}$$

The efficiency of the two controllers is illustrated in Figure 2, where they effectively bring the cart from an initial position of $y = 0.1$ to zero within approximately 10 seconds. Notably, when employing the SMC-based LMI controller, the oscillation range of the cart is reduced compared to the LQR controller, measuring 1.4m versus 2m, respectively. This observation highlights the superior performance of the SMC-based LMI controller in terms of minimizing oscillations and achieving smoother control of the vehicle's position.

A noticeable distinction between the two controllers is evident in the angular response of the pendulums. Figures 3 and 4

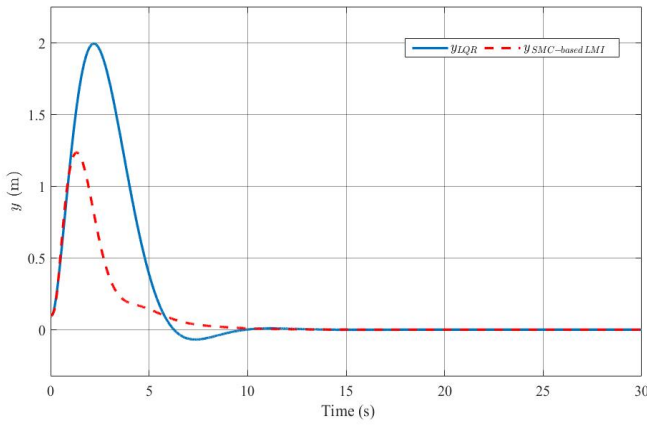


Figure 2. Distance of the cart y .

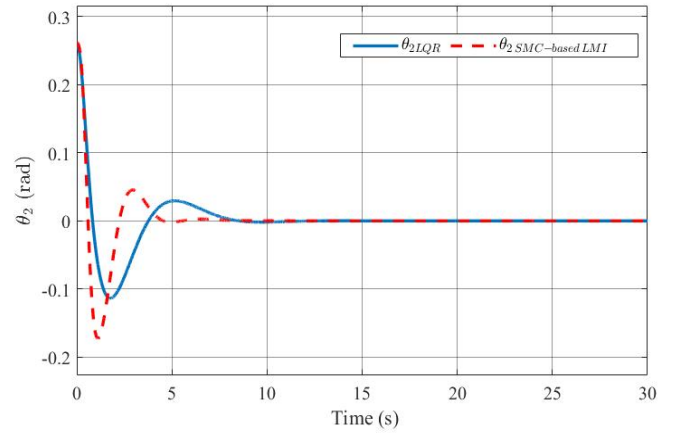


Figure 4. The angle position of second pendulum θ_2 .

demonstrate that both controllers successfully bring the pendulums to equilibrium from the same initial angle of $\frac{\pi}{12}$ (rad). While the oscillation amplitudes of the angles are larger when utilizing the SMC-based LMI controller compared to LQR, the time taken to reach the desired position is nearly twice as fast (5 seconds versus 9 seconds). This analysis leads to the conclusion that the SMC-based LMI controller offers superior control efficiency in comparison to LQR, despite the slightly larger oscillations in the angular response.

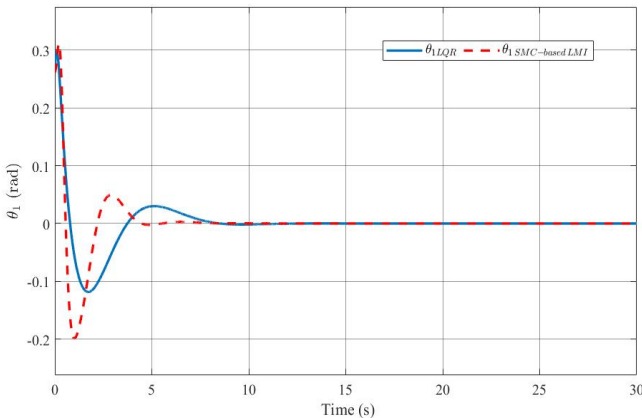


Figure 3. The angle position of first pendulum θ_1 .

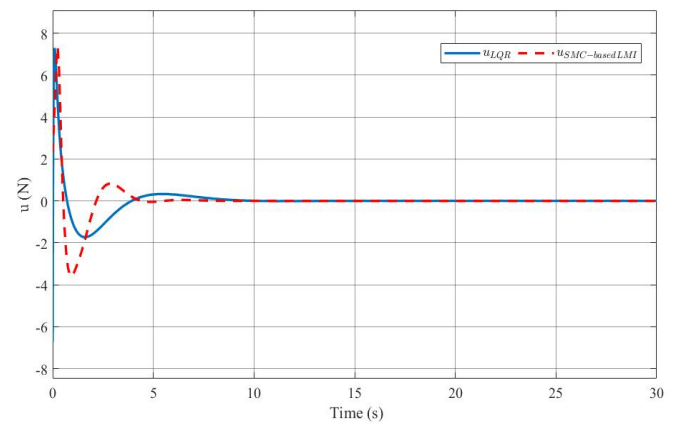


Figure 5. The control signal.

Figure 5 illustrates the control signal. The obtained results indicate that both the LQR control method and the SMC-based LMI method achieve effective stabilization of the double inverted pendulum. However, the SMC-based LMI method demonstrates a shorter pendulum stabilization time compared to the alternative method.

In order to assess the effectiveness of the two controllers, a disturbance component $d = 0.3\sin(t)$ has been introduced to the control signal. The simulation results depicted in Figures 6, 7, 8, and 9 demonstrate that despite the presence of disturbances, both controllers are capable of bringing the state variables close to the equilibrium point. While there is still observable oscillation of the state variables around the equilibrium position, it is noteworthy that values such as the maximum deviation of the vehicle's position or angle remain similar to those observed in the absence of disturbances. Remarkably, the SMC-based LMI controller exhibits superiority in this scenario, as evi-

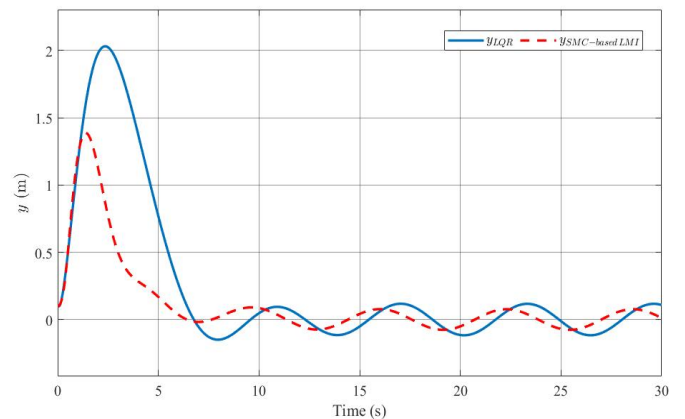


Figure 6. Distance of the cart y with disturbance.

denced by a smaller response time and reduced oscillation amplitude around the equilibrium point when compared to the LQR controller.

In order to gain a more comprehensive understanding of the enhancements in system performance achieved through the utilization of the SMC-based LMI controller in comparison to the LQR controller, we examine the performance index computed using equation (31):

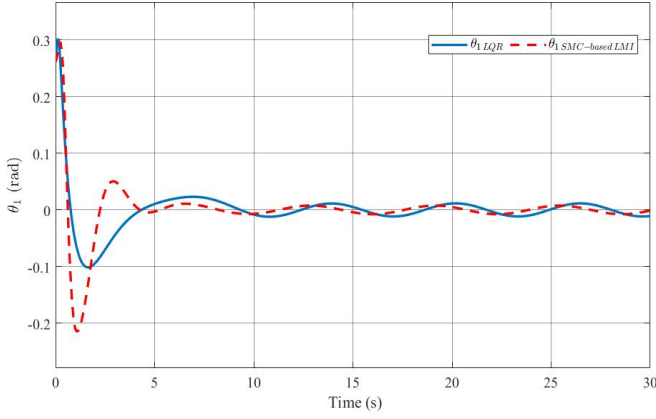


Figure 7. The angle position of first pendulum θ_1 with disturbance.

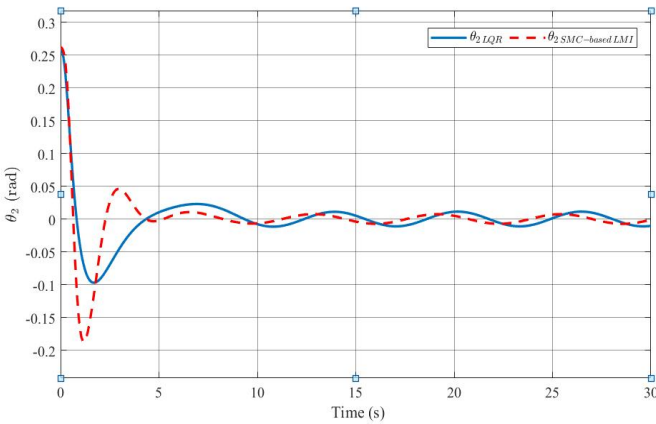


Figure 8. The angle position of second pendulum θ_2 with disturbance.

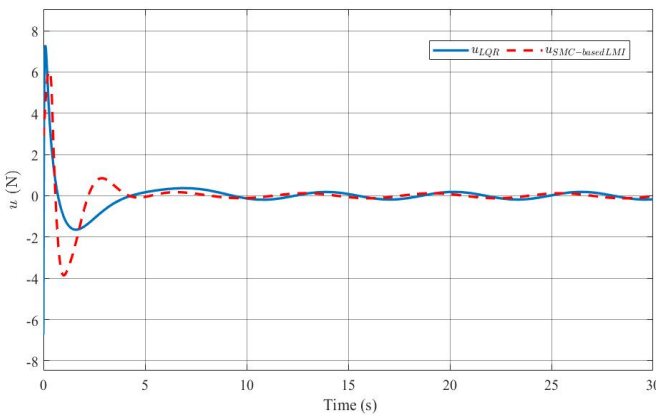


Figure 9. The control signal with disturbance.

$$Time_{performance} = \frac{t_{SMC}}{t_{LQR}} \times 100\% \quad (31)$$

where t_{SMC} and t_{LQR} are the settling times when using SMC-based LMI and LQR controllers, respectively. Table 2 presents the performance values of y , θ_1 and θ_2 .

When the system is subject to disturbance, the settling time value becomes unsuitable for comparison. Instead, the oscillation amplitude values of the state variables will be taken into

Table 2. Comparison in terms of settling time between two controllers.

	y	θ_1	θ_2
$Time_{performance}$	100%	49.28%	50.87%

Table 3. Comparison in terms of oscillation amplitudes between two controllers.

	y	θ_1	θ_2
$Amplitude_{performance}$	65.70%	67.26%	67.27%

consideration. Observing the relatively stable oscillation of the state variables around the equilibrium position between 10s and 20s, the amplitude values within this time period will be evaluated. The performance is calculated using equation (32).

$$Amplitude_{performance} = \frac{A_{SMC}}{A_{LQR}} \times 100\% \quad (32)$$

where A_{SMC} and A_{LQR} are the oscillation amplitudes when using SMC-based LMI and LQR controllers, respectively. The performance values of y , θ_1 and θ_2 are shown in Table 3.

6. Conclusion

In conclusion, this paper proposed a approach for stabilizing the highly nonlinear and unstable double inverted pendulum using a combination of sliding mode control and linear matrix inequality techniques. The SMC-based LMI controller exhibited superior performance compared to the linear quadratic regulator controller. The simulation results confirmed the effectiveness of the proposed controller, showcasing improved stability and achieving faster pendulum stabilization. The LMI-based approach offered computational efficiency and simplicity in implementation, making it a practical choice for real-world applications. Future research directions may include exploring adaptive control techniques and advanced optimization algorithms to further enhance control performance. The presented approach opens up new possibilities for controlling highly nonlinear and unstable systems, expanding their practical utility.

References

- [1] Jabbar, A., Malik, F. M., Sheikh, S. A. (2017). Nonlinear stabilizing control of a rotary double inverted pendulum: a modified backstepping approach. Transactions of the Institute of Measurement and Control, 39(11), 1721-1734.
- [2] Elkinany, B., Alfydi, M., Chaibi, R., Chalh, Z. (2020). TS fuzzy system controller for stabilizing the double inverted pendulum. Advances in Fuzzy Systems, 2020, 1-9.
- [3] Xu, X., Zhang, H., Carbone, G., Boubaker, O., Iriarte, R. (2017). Case studies on nonlinear control theory of the inverted pendulum. Inverted pendulum: from theory to new innovations in control and robotics, 225-262.
- [4] Sanjeeva, S. D., Parnichkun, M. (2022). Control of rotary double inverted pendulum system using LQR sliding surface based sliding mode controller. Journal of Control and Decision, 9(1), 89-101.
- [5] Singh, S., Swarup, A. (2021, June). Control of Rotary Double Inverted Pendulum using Sliding Mode Controller. In 2021 International Conference on Intelligent Technologies (CONIT) (pp. 1-6). IEEE.
- [6] Patil, M., Kurode, S. (2017, December). Stabilization of rotary double inverted pendulum using higher order sliding modes. In 2017 11th Asian Control Conference (ASCC) (pp. 1818-1823). IEEE.
- [7] Banerjee, R., Dey, N., Mondal, U., Hazra, B. (2018, March). Stabilization of double link inverted pendulum using LQR. In 2018 International Conference on Current Trends towards Converging Technologies (IC-CTCT) (pp. 1-6). IEEE.
- [8] Xia, X., Cheng, L. (2021). Habib, M. K., Ayankoso, S. A. (2020, December). Modeling and Control of a Double Inverted Pendulum using LQR with Parameter Optimization through GA and PSO. In 2020 21st

- International Conference on Research and Education in Mechatronics (REM) (pp. 1-6). IEEE.
- [9] Ratnayake, D. T., Parnichkun, M. (2020, July). LQR-based stabilization and position control of a mobile double inverted pendulum. In IOP Conference Series: Materials Science and Engineering (Vol. 886, No. 1, p. 012034). IOP Publishing.
 - [10] Tapia, A., Bernal, M., Fridman, L. (2017). Nonlinear sliding mode control design: An LMI approach. *Systems Control Letters*, 104, 38-44.
 - [11] Ali, M. A. S., Mehmood, K. K., Baloch, S., Kim, C. H. (2020). Wind-speed estimation and sensorless control for SPMSG-based WECS using LMI-based SMC. *IEEE Access*, 8, 26524-26535.
 - [12] Sun, Z., Wang, N., Bi, Y. (2015). Type-1/type-2 fuzzy logic systems optimization with RNA genetic algorithm for double inverted pendulum. *Applied Mathematical Modelling*, 39(1), 70-85.
 - [13] Maraslidis, G. S., Kottas, T. L., Tsipouras, M. G., Fragulis, G. F. (2021, September). A fuzzy logic controller for double inverted pendulum on a cart. In 2021 6th South-East Europe Design Automation, Computer Engineering, Computer Networks and Social Media Conference (SEEDA-CECNSM) (pp. 1-8). IEEE.
 - [14] Yadav, S. K., Sharma, S., Singh, N. (2012). Optimal control of double inverted pendulum using LQR controller. *International Journal of Advanced Research in Computer Science and Software Engineering*, 2(2).